LA-UR- 10-00979

Approved for public release;
distribution is unlimited.

Title: HEAT AND WATER TRANSPORT IN A POLYMER ELECTROLYTE FUEL CELL ELECTRODE

Author(s): P. P. Mukherjee
Devesh Ranjan
R. Mukundan
R. L. Borup

Submitted to: The 14th International Heat Transfer Conference (IHTC)

Form 836 (8/00)

The 14th International Heat Transfer Conference (IHTC)
August 7-13, 2010, Washington D.C., USA

IHTC14-22703

HEAT AND WATER TRANSPORT IN A POLYMER ELECTROLYTE FUEL CELL ELECTRODE

Partha P. Mukherjee[1]
Los Alamos National Laboratory
Los Alamos, NM, 87545, USA
[1]*Present Address*: Oak Ridge National Laboratory
PO Box 2008, Oak Ridge, TN 37831, USA

Devesh Ranjan
Department of Mechanical Engineering
Texas A&M University
College Station, TX 77843, USA

Rangachary Mukundan
Los Alamos National Laboratory
Los Alamos, NM, 87545, USA

Rodney L. Borup
Los Alamos National Laboratory
Los Alamos, NM, 87545, USA

ABSTRACT

In the present scenario of a global initiative toward a sustainable energy future, the polymer electrolyte fuel cell (PEFC) has emerged as one of the most promising alternative energy conversion devices for various applications. Despite tremendous progress in recent years, a pivotal performance limitation in the PEFC comes from liquid water transport and the resulting flooding phenomena. Liquid water blocks the open pore space in the electrode and the fibrous diffusion layer leading to hindered oxygen transport. The electrode is also the only component in the entire PEFC sandwich which produces waste heat from the electrochemical reaction. The cathode electrode, being the host to several competing transport mechanisms, plays a crucial role in the overall PEFC performance limitation. In this work, an electrode model is presented in order to elucidate the coupled heat and water transport mechanisms. Two scenarios are specifically considered: (1) conventional, Nafion® impregnated, three-phase electrode with the hydrated polymeric membrane phase as the conveyer of protons where local electro-neutrality prevails; and (2) ultra-thin, two-phase, nano-structured electrode without the presence of ionomeric phase where charge accumulation due to electro-statics in the vicinity of the membrane-CL interface becomes important. The electrode model includes a physical description of heat and water balance along with electrochemical performance analysis in order to study the influence of electro-statics/electro-migration and phase change on the PEFC electrode performance.

INTRODUCTION

In recent years, the polymer electrolyte fuel cell (PEFC) has emerged as a promising power source for a wide range of applications. The schematic of a typical PEFC is shown in Fig. 1. Despite tremendous recent progress in enhancing the overall cell performance, a pivotal performance/durability limitation in PEFCs centers on liquid water transport [1,2]. Liquid water blocks the porous pathways in the catalyst layer (CL) and gas diffusion layer (GDL) thus causing hindered oxygen transport to the reaction sites. This phenomenon is known as "flooding" and is perceived as the primary mechanism leading to the limiting current behavior in the cell performance. The cathode catalyst layer is a critical component in the fuel cell sandwich, where the electrochemical reaction takes place producing water and waste heat. The electrode, therefore, plays a major role in the PEFC water and thermal management, aimed at maintaining a delicate balance between reactant transport from the gas channels and water removal from the electrochemically active sites as well as ensuring membrane hydration with reduced protonic resistance.

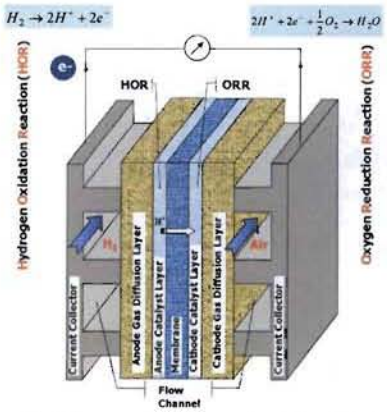

Figure 1: Schematic of a typical H_2/Air PEFC.

The state-of-the-art PEFC catalyst layer, with thickness ~ 10 μm, is a three-phase composite, and consists of: (1) ionomer, i.e. the ionic phase which is typically Nafion® to provide a passage for protons to be transported in or out, (2) Pt (platinum) nanoparticles as catalysts supported on highly porous carbon substrate as the electronic conductor, and (3) a porous network for the oxygen gas to be transferred in and product water out. This type of electrode relies on the electrochemically active area as the *three-phase interface*, shown in Fig. 2 using high resolution transmission electron microscope (TEM) image [3], for the electrochemical reaction to occur. Ensuring high catalyst utilization with very low Pt loading is a challenge in fabricating a *three-phase* electrode. The thin-film technique, originally proposed by Wilson [4] in his pioneering work in 1993 at Los Alamos National Laboratory, has been widely used in fabricating the three-phase catalyst layers. Gottesfeld and Zawodzinski [5] provided a good overview of the catalyst layer structure and functions. Litster and McLean [6] presented an overview of the different fabrication techniques for the conventional three-phase PEFC electrodes.

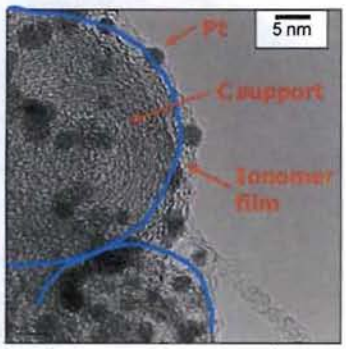

Figure 2: High resolution TEM image of a three-phase PEFC electrode [3].

In an effort to reduce Pt catalyst loading and improve catalyst utilization, recent advances in PEFC electrode development include the 3M® nanostructured thin film (NSTF) catalyst layer which obviates the use of carbon and ionomer [7,8]. Catalyst coated organic nano-whiskers, as shown in Fig. 3 [8], form the ultra-thin catalyst layer (~ 0.1 – 1μm) and the electrochemically active area is instead a *two-phase* interface for the electrochemical reaction to occur.

Figure 3: Scanning electron microscope (SEM) images (cross-section and plan views) of the ultra-thin NSTF electrode [8].

While the effects of flooding due to liquid water in the GDL and the flow field have been sufficiently studied [1], the role of CL flooding on the overall PEFC performance is yet to be clarified. Specifically, the capability of the CL as the only component in the entire fuel cell assembly in generating heat and the impact of the thermal effects on liquid water accumulation has not been studied. In this work, we present macrohomogeneous, 1-D models to elucidate heat and water transport scenarios in the state-of-the-art *three-phase* and ultra-thin *two-phase* PEFC electrodes.

NOMENCLATURE

a	electrochemically active area, m^2
c	concentration, mol/m^3
D	diffusivity, m^2/s
F	Faraday's constant
k	thermal conductivity, W/mK
R	universal gas constant, 8.134 J/molK
S	source/sink/saturation
T	temperature, ^0C

Greeks

ε	porosity
η	overpotential, V

Superscripts and Subscripts

eff	effective value
l	liquid
v	vapor

MODEL DESCRIPTION

Three-phase Electrode Model:

The transport model is based on the physical description of the water and heat balance in the conventional PEFC cathode CL with the *three-phase interface* as the electrochemical reaction site. The specific assumptions made in this model are [9]: (1) steady state; (2) incompressible and ideal gas mixture; (3) homogeneous and isotropic CL and GDL; (4) instantaneous and homogeneous evaporation of liquid water in the CL based on the saturation vapor pressure corresponding to local temperature; (5) a less hydrophobic CL than the GDL so that there is zero liquid water flux at the CL-GDL interface and only water vapor transport through the interface is allowed.

The liquid water transport through the porous CL can be described by Darcy's law:

$$-\frac{1}{V_m \mu^l}\frac{d}{dx}\left[k_{abs}k_r^l(S_r)\frac{dp_l}{dx}\right] = S_{ORR}^l - S_{evap}(S_r) \qquad (1)$$

In the above equation, V_m is the molar volume of water and μ_l the liquid water viscosity. k_{abs} is the absolute permeability of the porous medium and is only a function of the CL structure. k_r^l is the liquid water relative permeability which depends on the liquid water saturation and has been explained earlier. On the right hand side, S_{ORR}^l is the volumetric liquid water generation rate due to the ORR. Assuming that the reaction current is uniform throughout the CL of thickness δ_{CL}, the

volumetric liquid water generation rate corresponding to the fuel cell operating current density of I can be expressed as:

$$S_{ORR}^{I} = \frac{I}{2F\delta_{CL}} \tag{2}$$

F is the Faraday's constant. S_{evap} is the net volumetric evaporation rate.

Due to the less hydrophobic CL than GDL, considered in the present study, the liquid water cannot overcome the high capillary pressure barrier in the sufficiently hydrophobic GDL and hence the liquid water flux at the CL-GDL interface is assumed zero. Therefore only water vapor is allowed to transport through the GDL. Thus, the water vapor flux through the GDL, J_v^{GDL} can be expressed as:

$$J_v^{GDL} = D_{v,eff}^{GDL}\frac{dC_{sat}}{dx} = D_{v,eff}^{GDL}\frac{dC_{sat}}{dT}\frac{dT}{dx} \tag{3}$$

C_{sat} is the saturation vapor concentration corresponding to the local temperature, T.

The total heat generation rate in the CL can be approximately expressed as:

$$\dot{Q}_{tot} \approx (U_h - V_{cell})I \tag{4}$$

where U_h is the thermal potential of the ORR with the product water being liquid water and V_{cell} is the operating cell voltage. A simple estimate based on the total heat generation reveals that the evaporation rate can ideally supersede the rate of liquid water production from the ORR. However, due to the high thermal conductivity of the gas diffusion layer, only a fraction of the total heat generated in the CL can be utilized to evaporate the liquid water and the rest is conducted away through the GDL. The net volumetric evaporation rate in the CL can, therefore, be expressed in terms of the total heat generation rate as:

$$S_{evap}(S_r) = \frac{\beta(S_r)\times\dot{Q}_{tot}}{h_{fg}} \tag{5}$$

β refers to the *heat partition factor* and corresponds to the fraction of the total heat generation rate actually available for the evaporation of liquid water in the CL. Considering the heat balance in the CL and GDL as well as the vapor diffusion through the GDL, the heat partition factor can be uniquely defined in terms of the GDL thermal conductivity and the saturation vapor concentration depending on the fuel cell operating temperature as the following:

$$\beta_{avg} = \frac{h_{fg}D_{v,eff}^{GDL}\dfrac{dC_{sat}}{dT}}{k_{GDL}^{*} + h_{fg}D_{v,eff}^{GDL}\dfrac{dC_{sat}}{dT}} \tag{6}$$

Voltage Loss in the Presence of Liquid Water:

Liquid water blocks the porous network causing impeded oxygen diffusion to the active sites. The blockage of oxygen diffusion can be described by the effective oxygen diffusivity, $D_{O_2}^{eff}$, with a decreasing effective pore volume fraction available for transport.

$$D_{O_2}^{eff} = D_{O_2}(T,P)[\varepsilon_{CL}(1-S_r)]^m \tag{7}$$

where D_{O_2} is the diffusion coefficient of oxygen in air corresponding to the operating temperature, T and operating pressure, P and ε_{CL} the CL porosity.

The catalytic surface coverage effect due to liquid water can be expressed via a decreasing electrochemically active area (ECA).

$$a^{eff} = a(1-S_r)^n \tag{8}$$

where a is the intrinsic ECA available for electrochemical reaction. The values of the exponents, m and n, in the effective oxygen diffusivity and ECA expressions above, respectively, depend on the underlying CL morphology and liquid water transport.

The electrochemical kinetics is described by the Tafel equation.

$$j = i_0(T)a(1-S_r)^n\frac{c_{O_2}^{CL}}{c_{O_2}^{ref}}\exp\left(-\frac{\alpha_c F}{RT}\eta_c\right) \tag{9}$$

Assuming that the reaction current is uniform throughout the CL, the oxygen concentration distribution along the CL thickness can be described by a quadratic distribution as:

$$\frac{\partial}{\partial x}\left(D_{O_2}[\varepsilon_{CL}(1-S_r)]^m\frac{\partial c_{O_2}^{CL}}{\partial x}\right) = \frac{j}{4F} = \frac{I}{4F\delta_{CL}} \tag{10}$$

Assuming a zero oxygen flux at the membrane-CL interface and a value of oxygen concentration at the CL-GDL interface estimated from an assumed linear oxygen concentration distribution along the GDL thickness, Eq. (16) can be solved analytically to obtain the local concentration of oxygen in the CL as a function of that in the flow channel. That is:

$$c_{O_2}^{CL}(x) = c_{O_2}^{Ch} - \frac{I}{4F}\left(\frac{\delta_{GDL}}{D_{O_2}\varepsilon_{GDL}^{1.5}}\right) - \frac{I}{4F}\frac{\delta_{CL}\left[1-\left(\dfrac{x}{\delta_{CL}}\right)^2\right]}{D_{O_2}[\varepsilon_{CL}(1-S_r)]^m} \tag{11}$$

where $c_{O_2}^{Ch}$ is the oxygen concentration in the flow channel pertaining to the channel inlet pressure and cell operating temperature which physically corresponds to a large stoichiometric flow rate.

Taking the average of the oxygen concentration in the cathode CL and substituting into Eq. (9), the cathode overpotential can be obtained as a function of the current density and the average liquid water saturation in the cathode CL. That is:

$$\eta_c = -\frac{RT}{\alpha_c F}\ln\left(\frac{I}{a(1-S_r)^n i_0 \delta_{CL}}\cdot\frac{c_{O_2}^{ref}}{c_{O_2}^{Ch} - \frac{I}{4F}\left(\frac{\delta_{GDL}}{D_{O_2}\varepsilon_{GDL}^{1.5}} + \frac{2\delta_{CL}}{3D_{O_2}[\varepsilon_{CL}(1-S_r)]^n}\right)}\right) \quad (12)$$

In the above equation, the first term within the logarithmic expression corresponds to the effect of liquid water in the ECA reduction and the second term represents the hindered oxygen transport effect.

Two-phase Electrode Model:

The ultra-thin *two-phase* catalyst layer is assumed to consist of Pt particles on inert support material and pores. Reduced thickness, enhanced electrochemically active area and hydrophilic characteristics make the ultra-thin electrode prone to excessive flooding due to liquid water on the cathode side, as experimentally evidenced by Debe [7]. Based on the modeling description by Eikerling and co-workers [10], the following assumptions are specifically made for the macrohomogeneous, 1-D model: (1) steady state and isothermal operation; (2) uniform electronic potential since the CL is very thin and the electronic conductivity of Pt particles sufficiently high; (3) pores are completely filled with liquid water and distribution of water stationary with respect to the solid matrix (Pt/support); (4) convective transport being negligible, oxygen and protons transport in the liquid water is governed by Fickian diffusion; and (5) the effect of phase change due to heat generation in the CL is not considered.

The proton transport in liquid water filled pores via migration and diffusion along with the proton depletion sink term due to electrochemical reaction is governed by the Nernst-Planck equation:

$$-\frac{d}{dz}\left(D_{H^+}^{eff}\frac{dc_{H^+}}{dz} + \frac{F}{RT}c_{H^+}\frac{d\eta}{dz}\right) = -\frac{a_{eff}\, j}{F} \quad (13)$$

where c_{H^+} is proton concentration, $D_{H^+}^{eff}$ the effective proton diffusivity in the liquid water filled pores, a_{eff} the effective electrochemically active area, j the reaction current density, and η is the cathode overpotential. It is worth noting that the proton transport in the ionomer phase in the conventional three-phase electrode ensures electro-neutrality and hence Ohm's law describes the ion transport under the influence of the potential gradient.

The reaction current density, j, is given by [10]:

$$j = -i_0\left(\frac{c_{O_2}}{c_{O_2}^{ref}}\right)\left(\frac{c_{H^+}}{c_{H^+}^{ref}}\right)\exp\left(-\frac{\alpha_c F}{RT}\eta\right) \quad (14)$$

where i_0 is the exchange current density, c_{O_2} is the oxygen concentration, $c_{O_2}^{ref}$ and $c_{H^+}^{ref}$ are reference oxygen and proton concentrations, respectively.

In Eq. (13), the first term is the diffusion due to proton concentration gradient and the second term is proton migration due to the electric field. The closure between the proton concentration and cathode overpotential is given the Poisson equation:

$$-\frac{\varepsilon\varepsilon_0}{F}\frac{d^2\eta}{dz^2} = c_{H^+} \quad (15)$$

where ε is the relative dielectric constant of water in pores and ε_0 is the permittivity of vacuum.

Oxygen diffusion in the liquid water filled pores is given by:

$$-D_{O_2}^{eff}\frac{d^2 c_{O_2}}{dz^2} = -\frac{a^{eff}\, j}{4F} \quad (16)$$

The model domain and the pertinent boundary conditions are described in Fig. 4.

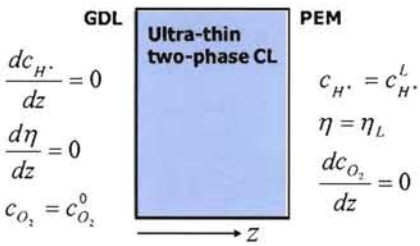

Figure 4: Schematic of the ultra-thin two-phase CL model domain and the boundary conditions.

RESULTS AND DISCUSSION

Three-phase Conventional Electrode:

Figure 5 shows the liquid water saturation distributions in the CL for different values of heat partition factors at 60°C cell operating temperature and 0.6V cell voltage. It is to be noted that the transport calculations presented in this work are based on a fully hydrophilic CL structure. It is evident from Fig. 5 that increasing value of the heat partition factor promotes higher utilization of the available heat generated in the CL for enhanced evaporation and leads to the reduction of the liquid water saturation level in the CL. The lowest liquid water saturation level of 5% is set in the current model which corresponds to the highest heat partition factor. From the figure it is observed that the liquid water saturation distribution is quite uniform along the CL thickness leading to apparently benign saturation gradient. This indicates that the effect of evaporation is indeed dominant as compared to the capillarity effect in the overall liquid water transport and distribution in the hydrophilic and only 10 μm thick CL considered in this study.

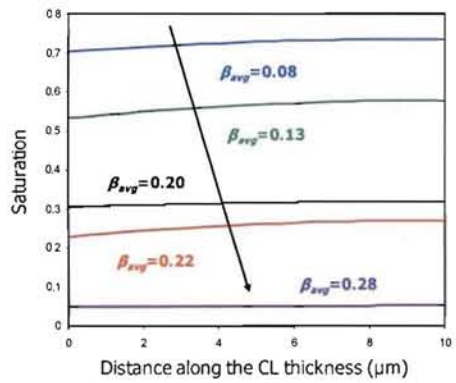

Figure 5: Liquid water saturation distributions along the thickness of the three-phase CL with different heat partition factors.

Figure 6 shows the effect of the fuel cell operating temperature on the liquid water saturation distributions in the CL for cell voltage of 0.6V and the GDL thermal conductivity of 1.5 W/mK. Since the saturation vapor pressure is a strong function of the temperature, with elevated temperature the heat partition factor increases leading to a higher portion of the heat generated actually available for evaporation in the CL. This enhanced evaporation results in significantly lower liquid water saturation level at 70°C as compared to that at 25°C.

$k^{*}_{GDL} = 1.5$ W/mK

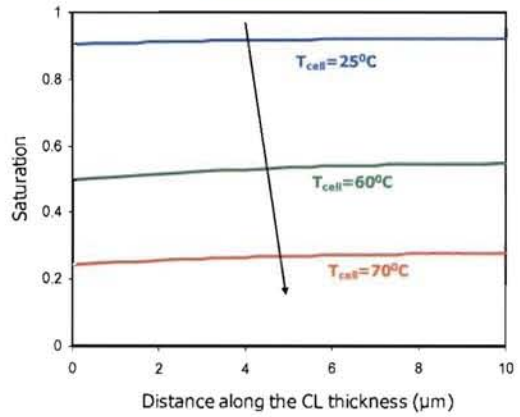

Figure 6: Liquid water saturation distributions along the thickness of the three-phase CL for different cell operating temperatures and with GDL thermal conductivity of 1.5 W/mK.

Figure 7 depicts the effect of higher GDL thermal conductivity on the liquid water saturation distributions in the CL for different cell operating temperatures. Higher GDL thermal conductivity allows a larger fraction of the heat generated in the CL to be conducted away through the diffusion medium, which leads to lower heat partition factors and subsequently diminished evaporation capability of the CL. The lower evaporation rate manifests in terms of an elevated liquid water saturation level even at sufficiently high operating temperature, e.g. at 70°C as compared to that shown in Fig. 6.

$k^{*}_{GDL} = 10$ W/mK

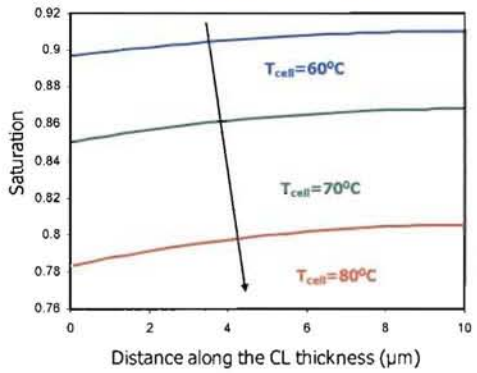

Figure 7: Liquid water saturation distributions along the thickness of the three-phase CL for different cell operating temperatures and with GDL thermal conductivity of 10 W/mK.

Figure 8 shows the effect of the cell operating temperature on CL flooding and the subsequent CL voltage loss with the GDL thermal conductivity of 1.5 W/mK. As it has been already explained, higher temperature leads to enhanced evaporation rate and results in lower liquid water saturation level in the CL. At lower temperature, e.g. 25°C, due to the ineffective evaporation, there is a surge in the overall liquid water saturation to a detrimental level, which manifests in terms of a severe voltage loss and exhibits the onset of the limiting current behavior at a significantly low current density. While at higher temperature, e.g. at 60°C, due to the lower liquid water saturation level the voltage loss penalty from the CL flooding alone does not lead to the catastrophic limiting current behavior in the global cell performance curve.

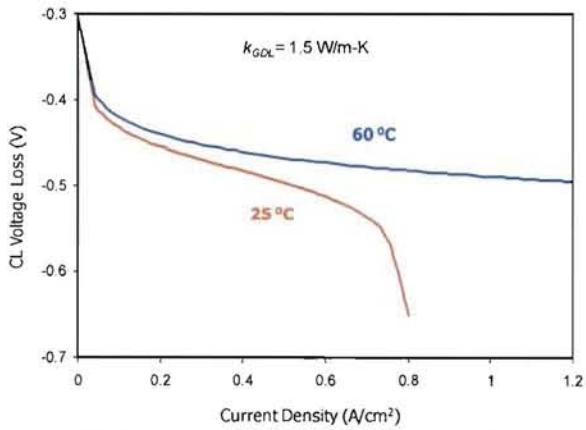

Figure 8: Effect of the operating temperature on the three-phase CL voltage loss.

Two-phase Ultra-thin Electrode:

Figure 9 show the proton concentration (Fig. 9a) and cathode overpotential (Fig. 9b) distributions normalized with the respective values specified at the CL/PEM interface along the thickness in a 0.4 μm two-phase CL and at 1.0 A/cm^2. The proton concentration exhibits an accumulation near the CL/PEM interface, while the overpotential shows an increase

toward the CL/GDL interface. The strikingly high concentration of protons in the immediate vicinity of the CL/PEM interface suggests the formation of an electric double layer between the water filled pores in the CL and the electro-neutral bulk membrane. The effect of the double layer dominates the proton migration term as compared to the rather facile effects owning to fast proton diffusion in water and a small electrochemical reaction sink term, described in Eq. (13). The double layer formation and hence the electro-statics effect becomes the limiting factor. Higher proton concentration also reflects in a lower overpotential near the CL/PEM interface and gradual increase toward the CL/GDL interface for an imposed current density.

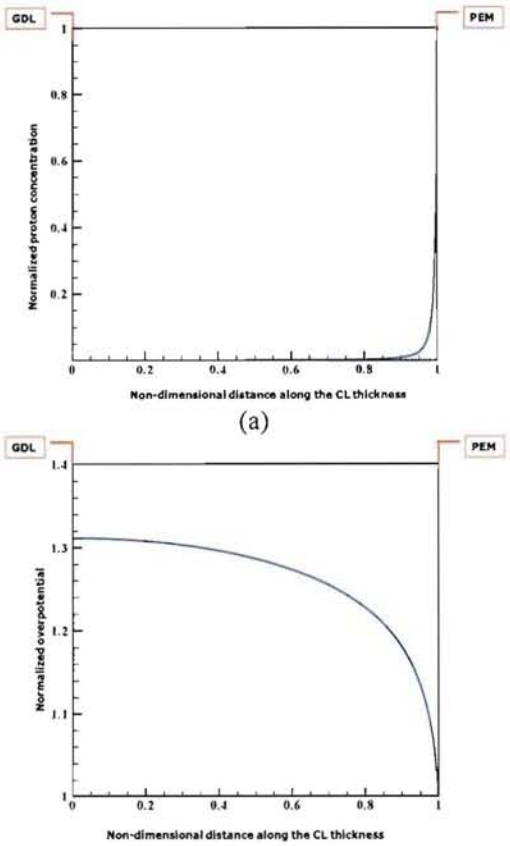

Figure 9: Normalized proton concentration (a) and overpotential (b) distributions along the thickness of a 0.4 μm two-phase CL.

The effect of CL thickness on the proton concentration and overpotential is depicted in Fig. 10. Calculations are performed for four different CL thickness values (0.1, 0.2, 0.4, 0.6 μm). It is evident that with the decrease in the CL thickness, the proton concentration distribution becomes relatively uniform over the thickness and somewhat relaxes the limiting behavior owing to the double layer formation and charge accumulation near the CL/PEM interface. The decrease in CL thickness and hence the uniformity of proton concentration distribution also show a decrease in the overpotential growth toward the CL/GDL interface.

The importance of double layer overlapping in charge accumulation and the effect of evaporation on the ultra-thin electrode performance are currently underway.

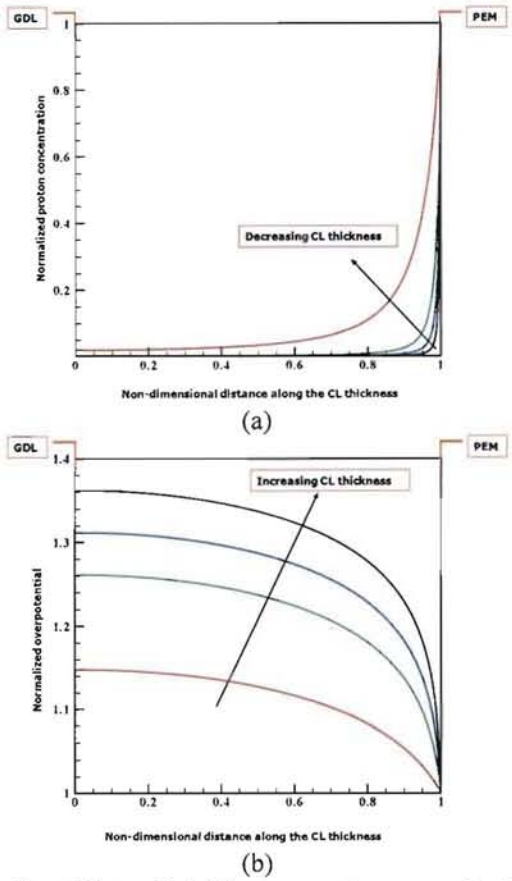

Figure 10: Effect of thickness on the normalized proton concentration (a) and overpotential (b) distributions in the two-phase CL.

CONCLUSIONS

In this work, the heat and water transport scenarios in conventional three-phase and ultra-thin two-phase PEFC electrodes are elucidated. The transport model for the three-phase CL is based on the physical description of heat and water balance. The evaporation is a critical factor affecting the CL performance. The cell operating temperature and the GDL thermal conductivity play significant roles in CL flooding. Higher temperature promotes evaporation while higher GDL thermal conductivity renders insufficient evaporation in the CL. In the two-phase ultra-thin electrode model, proton transport in liquid water filled pores is considered. The double layer formation is the dominant factor and significantly affects the proton concentration distribution. Lowering the CL thickness promotes proton concentration uniformity and lowers cathode overpotential. Detailed studies of water and thermal transport in

these two disparate electrode scenarios along with experimental performance evaluation are currently underway.

ACKNOWLEDGMENTS

Financial support from Los Alamos National Laboratory LDRD program and DOE EERE Fuel Cell Technologies Program is gratefully acknowledged.

REFERENCES

1. C. Y. Wang, *Chem. Rev.*, **104**, 4727 (2004).
2. R. L. Borup *et al.*, *Chemical Reviews*, **107**, 3904 (2007).
3. K. L. Moore and K. S. Reeves, DOE Hydrogen Program Annual Merit Review Proceedings, Arlington, VA, USA, May 23-26 (2005).
4. M. S. Wilson, U.S. Pat. No. 5, 234, 777 (1993).
5. S. Gottesfeld and T. A. Zawodzinski, in *Advances in Electrochemical Science and Engineering*, C. Tobias, Editor, Vol. 5, Wiley and Sons, New York (1997).
6. S. Litster and G. McLean, *J. Power Sources*, **130**, 61 (2004).
7. M. K. Debe, in: *Handbook of Fuel Cells—Fundamentals Technology and Applications*, Eds. W. Vielstich, A. Lamm, and H.A. Gasteiger, John Wiley & Sons, Chapter 45, (2003).
8. M. K. Debe, A. K. Schmoeckel, G. D. Vernstrom, and R. Atanasoski, *J. Power Sources*, **161**, 1002 (2006).
9. P. P. Mukherjee, *Ph.D. Dissertation*, Pennsylvania State University (2007).
10. Q. Wang, M. Eikerling, D. Song, and Z. S. Liu, *J. Electrochem. Soc.*, **154**, F95 (2007).